Check for updates

Moisture legacy effects shape vegetation productivity across East Asia ecosystems, 2001-2020

Pingping Zheng[1], Mark Henderson[2], Binhui Liu[1]*,
Mingyang Chen[1], Kexin Deng[1], Ruiting Gu[1] and Xiaojing Gong[1,3]

[1]College of Forestry, The Northeast Forestry University, Harbin, China, [2]Mills College, Northeastern University, Oakland, CA, United States, [3]Changzhou Architectural Research Institute Group Co., Ltd., Changzhou, China

This study investigated spatiotemporal patterns of growing season gross primary productivity (GPP_{GS}) across three vegetation types in mid-to-high latitude East Asia from 2001-2020.Growing season parameters and GPP were extracted from MODIS satellite data and combined with meteorological data to examine climate-vegetation relationships through trend analysis and correlation methods. GPP_{GS} increased significantly overall (4.12 gC/m2/yr), with deciduous broad-leaved forest (DBF) having highest productivity (1035.52 gC/m2), followed by deciduous needle-leaved forest (DNF) (830.83 gC/m2) and grassland (800.62 gC/m2). A critical divergence occurred around 2014, when grassland and DNF growth rates declined substantially while DBF maintained steady increases. Phenological factors showed limited explanatory power for GPP variations, albeit GPP are sensitive to vegetation peak growth time for all three vegetation types. Climate analysis identified relative humidity (RH) as the dominant driver, with the previous year's growing season RH showing around 35.91% stronger positive correlations than current year values across all vegetation types; the difference is highest in DNF and the least in grassland. We conclude that the legacy effects of atmospheric moisture conditions explained the 2014 divergence, highlighting the increasing importance of water availability under global warming. Increases in atmospheric dryness accompanied by temperature increases will affect vegetation carbon storage and the societal-economic services provided by these ecosystems.

KEYWORDS

gross primary productivity, vegetation phenology, climate change, relative humidity, soil moisture

1 Introduction

Gross Primary Productivity (GPP) of terrestrial ecosystems refers to the amount of organic matter fixed by green plants per unit area per unit time through photosynthesis and a series of internal physiological processes (Anav et al., 2015; Campbell et al., 2017; Hilty et al., 2021). GPP is directly related to the strength of the carbon sink of terrestrial

vegetation and represents the largest carbon flux between terrestrial ecosystems and the atmosphere (Zhao et al., 2005; Beer et al., 2010; Hu et al., 2018).

Extensive research has confirmed that terrestrial plant ecosystems in mid- to high-latitude regions play a crucial role in regulating the global carbon cycle and atmospheric CO_2 concentrations (Dang et al., 2023). In East Asia, these latitudes have seen rapid warming in recent decades and are home to vegetation with high sensitivity to climate change (Lv et al., 2023; Chen et al., 2024b). Studying the pattern of change in GPP and its connection with the changing climate will help to improve our understanding of the carbon cycle.

While most of the previous studies qualitatively or quantitatively analyzed the direct influence of either meteorological factors or phenology on the annual GPP dynamics (Wang et al., 2021; Wu et al., 2021), fewer studies have investigated combined the influence of climate and vegetation phenology simultaneously on the magnitude of changes in vegetation productivity (Fu et al., 2018; Xu et al., 2021). In addition, current research on the relationship between vegetation growth and climatic factors focuses mainly on climatic factors such as temperature and precipitation (Hu et al., 2021; Liao et al., 2024), and most of them ignoring the possible differences in the response of different vegetation types. There is a need for studies to simultaneously investigate the combined influence of climate and vegetation phenology on changes in vegetation productivity and to consider the possible differences in response among different vegetation types. Therefore, for this study we use MOD17A2HGF.061 GPP data from 2001–2020 along with meteorological data to investigate the spatial and temporal characteristics of growing season cumulative gross primary productivity (GPP_{GS}) of different vegetation types and their responses to climate change and vegetation phenology in the middle to high latitudes of East Asia.

1.1 Factors influencing GPP

Spatiotemporal variations in global terrestrial GPP are related to climatic conditions, Photosynthetically Active Radiation (PAR, as a source of energy for photosynthesis), vegetation types, and land use patterns (Ichii et al., 2005; Ahlström et al., 2015; Yao et al., 2018; Xie et al., 2021; Chen et al., 2022). Among climatic factors, temperature and precipitation have been shown to be critical in the dynamics of vegetation GPP (Chen et al., 2021; Meng et al., 2023b; Xu et al., 2023).They impact carbon absorption directly by altering photosynthetic rates and water use efficiency, or indirectly through modifying the rhythm of plant phenology (Hatfield and Dold, 2019; Shi et al., 2022; Xiao et al., 2023).

Other climate indicators such as air and soil moisture conditions also play important roles. Soil moisture (SM) determines the amount of water that can be drawn by plant roots, and its fluctuations can affect leaf structure and root growth, thereby influencing vegetation photosynthesis (Green et al., 2019; Liu et al., 2020b; Xu et al., 2024). In terms of air moisture

conditions, elevated vapor pressure deficit (VPD) significantly reduces stomatal conductance and limits the actual photosynthetic rate, thereby reducing vegetation productivity (López et al., 2021). Similarly, excessively low relative humidity (RH) causes the closure of plant leaf stomata and a reduction in the amount of carbon dioxide available to the plant, which in turn leads to a reduction in the efficiency of photosynthetic carbon fixation (Zhao et al., 2019; López et al., 2021). In either case, a shortage of water can limit plant growth and ecosystem carbon fluxes, but there are some differences and commonalities between the effects of VPD and RH. Firstly, it has been found that climate warming has a minimal effect on RH, but VPD is increasing exponentially, suggesting that VPD and RH do not change synchronously (Held and Soden, 2000). Secondly, VPD reflects the combined changes in air temperature and relative humidity: high temperatures and stable RH lead to higher VPD, which increases plant water demand and reduces carbon assimilation rate (Zhang et al., 2021). Compared with RH, VPD more directly impacts the water use efficiency of trees, thereby affecting vegetation productivity (Sato et al., 2015; Li et al., 2023). With global warming, if water vapor pressure increases at a proportional rate with saturated water vapor pressure (which is temperature-dominated), the VPD will increase, but RH more likely remain stable. Therefore, VPD may not change in synchrony with RH, with RH lagging behind VPD.

GPP is the cumulative rate of gross plant photosynthesis over time. Over the course of the growing season and from year to year, changes in vegetation phenology may induce GPP changes (Xia et al., 2015). In general, vegetation phenology directly affects surface energy exchange, water cycle, and terrestrial carbon cycle,and plays a critical role in determining the duration of canopy photosynthetic activity, and drives ecosystem carbon sequestration (Richardson et al., 2010; Wang et al., 2017). As such, climate change not only affects GPP directly, but may also modulate GPP through altering phenology (Baldocchi et al., 2018). In addition, the effects on vegetation productivity through climate change and phenology changes may vary across different regions or vegetation types (Abbas et al., 2021). For example, the relative impacts of climate change and phenological changes on grassland productivity in the Tibetan Plateau vary with grassland type (Xiao et al., 2023). An earlier start to the growing season (SOS) in spring and higher photosynthetic peaks in summer was found to alter the seasonal pattern of vegetation productivity in the middle and lower reaches of the Yangtze River, China (Yang et al., 2024). A recent study also demonstrated that, in the mid- to high-latitude regions of the Northern Hemisphere, early SOS and a delayed end of the growing season (EOS) contributed to the increase in forest GPP in spring and autumn, respectively (Wang et al., 2025). These findings confirm that changes in phenology, serving as a sensitive and direct indicator of climate change, also influence the seasonal and annual dynamics of GPP (White et al., 2009), and that the effects of phenology and climatic factors, while not completely synchronized, play direct or indirect roles in the variation of GPP (Yang et al., 2017).
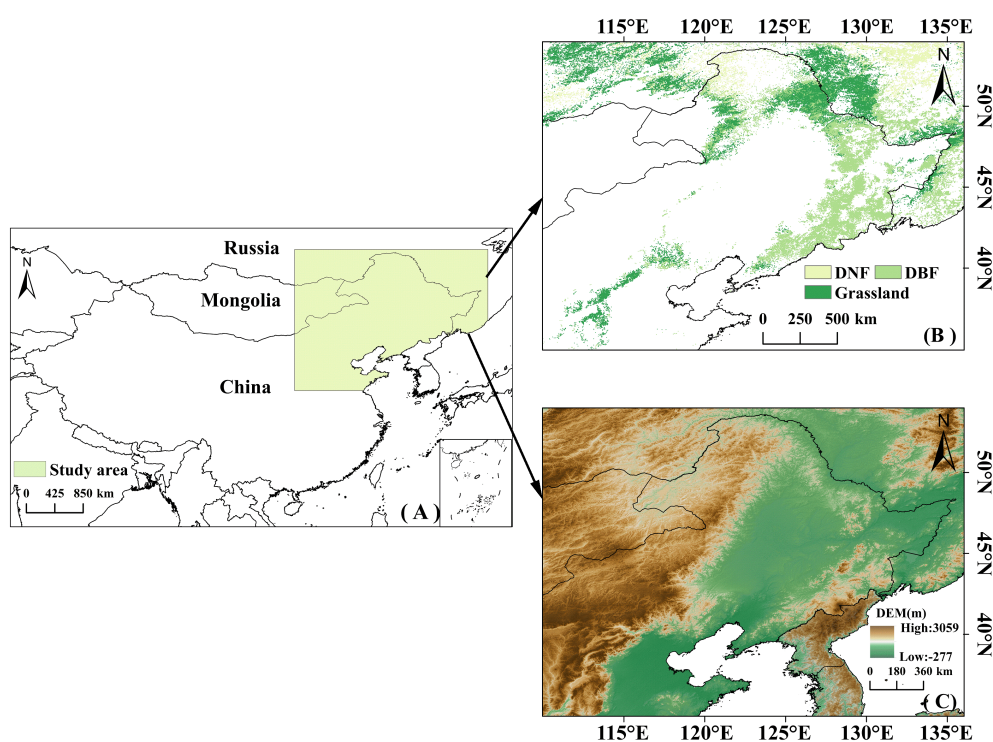
FIGURE 1
(A) Schematic map of the study area; **(B)** Distribution of the three vegetation types in the study area; **(C)** Elevation map of the study area.

1.2 Study objectives

The objectives of this study include (1) investigating the spatial and temporal variation of GPP_{GS} for different vegetation types in the mid-to-high latitude of East Asia; (2) analyzing the relationships between GPP_{GS} and growing season climatic variables—maximum temperature (T_{max}), minimum temperature (T_{min}), photosynthetically active radiation (PAR), precipitation (P), relative humidity (RH), soil moisture (SM), and Vapor Pressure Deficit (VPD)—as well as phenological variables; and (3) determining the dominant factors driving temporal changes in GPP_{GS} among climate and phenological indicators for grassland, deciduous needleleaf forests, and deciduous broadleaf forests during the period of 2001-2020. By elucidating the intricate relationship between vegetation GPP and climate change in this region, our findings offer valuable insights for predicting shifts in vegetation productivity under future global warming scenarios.

2 Materials and methods

2.1 Study area

The study area is located in the middle and high latitudes of northeastern Asia (35° to 54°N, 110° to 135°E), primarily including Northeast China and parts of Russia (Figure 1A). This region has experienced rapid temperature increases over the past few decades (IPCC, 2014). The topography is characterized by higher elevations

in the west and lower in the east (Figure 1C). The majority of the study area belongs to the temperate continental climate zone, whereas the southeastern coastal areas are characterized by a temperate monsoon climate; precipitation and temperature increase from northwest to southeast. With complex topography and spatial variability in climate conditions, the study area's vegetation is highly sensitive to climate change (Wang et al., 2022a; Chen et al., 2024b). The study area includes three vegetation types: grasslands in the north, south, and west; deciduous broadleaf forests (DBF) in the east; and deciduous needleleaf forests (DNF) in the north (Figure 1B). Excluding other land cover types such as agriculture, desert, or urban uses, or areas that changed during the study period, DBF, grasslands, and DNF make up 47.09%, 44.23%, and 8.68%, respectively, of the study area.

2.2 Datasets

2.2.1 Phenology and GPP

This study utilized two Moderate Resolution Imaging Spectroradiometer (MODIS) products with a spatial resolution of 500m covering the years from 2001 to 2020. These products, released by the U.S. National Aeronautics and Space Administration (NASA) (https://www.earthdata.nasa.gov). included annual vegetation phenology data (MCD12Q2) and 8-day GPP data (MOD17A2HGF.061). The vegetation phenology products were derived from the time series of Normalized

Difference Vegetation Index (NDVI). Four phenological indicators were selected for analysis: SOS, the start of the growing season; POS, the time of the peak growing season; EOS, the end of the growing season; and LOS, the length of the growing season. Additionally, the 8-day GPP were converted to months, and the cumulative GPP for the growing season of each year (April-October) was computed (hereafter denoted as GPP_{GS}) to obtain the 20-year GPP_{GS} time series (Hu et al., 2021).

2.2.2 Meteorological data

Meteorological data were obtained from the climate dataset produced by the National Tibetan Plateau Data Center (https://data.tpdc.ac.cn/), with a spatial resolution of 1 km covering the period from 1901 to 2023. From this dataset, we obtained climate data include maximum temperature (T_{max}), minimum temperature (T_{min}), soil moisture (SM) and precipitation (P). Photosynthetically Active Radiation (PAR) and Relative Humidity (RH) were obtained from the National Earth System Science Data Centre (https://www.geodata.cn/main/), with the PAR dataset spanning the period of 2000–2022 with a spatial resolution of 0.05°, whereas the RH dataset covers the period of 2000–2020 with a spatial resolution of 1 km. We obtained all meteorological data on a monthly scale for the period 2001–2020 and calculated the growing season (April-October) average, except for precipitation, which was calculated as the cumulative value for the growing season.

To obtain unified resolution, we resampled the meteorological data to a 500m resolution, consistent with the GPP data resolution, using a NEAREST interpolation method commonly adopted by prior studies (Zu et al., 2018; Mei et al., 2021; Shen et al., 2024b).

2.2.3 Other data

The MCD12Q1 dataset (https://ladsweb.modaps.eosdis.nasa.gov) provides the annual distribution of different land cover types globally at 500 m spatial resolution. The land cover types in the study area were classified into DBF, DNF and grassland by taking the areas that did not change between 2001 and 2020 (Figure 1B). The digital elevation model (DEM) data were obtained from the geospatial data cloud (https://www.gscloud.cn/search), with a resolution of 90 m.

2.3 Methods

2.3.1 Extraction of vegetation phenology parameters

In this study, the dynamic thresholding method of S-G filtering method was used to extract vegetation phenology parameters using TIMESAT in MATLAB software. Firstly, in order to remove the random noise in the time series, the MODIS data were smoothed by S-G filtering, which has been widely used for data smoothing and noise reduction as it eliminates the noise while maintaining the shape and width of the original signal (Jeong et al., 2011). Next, the dynamic thresholding method was used to extract vegetation phenology parameters (Jonsson and Eklundh, 2002). This method

is based on the relative amplitude of the whole time series to obtain the vegetation phenology period information. According to the criteria of former related research, define the start of the growing season (SOS) and the end of the growing season (EOS) as the dates of the first crossing the 30% NDVI amplitude and the last crossing the 50% NDVI amplitude, respectively (Piao et al., 2020). The length of the growing season (LOS) was obtained by subtracting the end date of the growing season from the start date of the growing season. The time when NDVI reaches its maximum amplitude marks the peak of vegetation growth (POS), representing the date on which vegetation photosynthesis reaches its maximum (Liu et al., 2025). The dynamic threshold model is as follows (Myneni et al., 1997; Sisheber et al., 2022):

$$NDVI_{thr} = (NDVI_{max} - NDVI_{min}) \times C$$

where $NDVI_{thr}$ is the threshold value, $NDVI_{max}$ is the maximum value in the ascending phase, $NDVI_{min}$ is the minimum value in the decreasing phase, and C is the coefficient.

2.3.2 Trend analysis

To detect temporal trends of climatic variables, vegetation phenology, and annual GPP over the past 20 years and their corresponding significance, the non-parametric Sen's slope method and Mann-Kendall trend analysis were used (Sen, 1968). We analysed the data on a raster scale using Matlab R2024a software. The slope was calculated by the following equation:

$$Slope = \text{Median}\left[\frac{X_j - X_i}{j - i}\right], \forall\ 1 \leq i \leq j \leq n$$

where x_j and x_i represent the values at times i and j, and n represents the length of the time series data. When Slope is positive, it indicates that the variable has an upward trend; when Slope is negative, it indicates that the variable has a downward trend; the larger the absolute value of Slope, the larger the magnitude of the change trend. An upward slope suggests a delay in the phenological period and an increase in GPP accumulation and climate factors. Conversely, a downward slope suggests an advancement in the phenological period and a decrease in GPP accumulation and climate factors.

To analyze temporal variation, we applied a nine-point binomial filter with reflected ends to smooth out year-to-year variations and show the longer-term trend.

2.3.3 Correlation analysis

We calculated the correlation between phenological and climatic factors and GPP_{GS} using correlation analysis. The correlation coefficient r was calculated by the following equation:

$$r = \frac{\sum_{i=1}^{n}(x_i - \bar{x})(y_i - \bar{y})}{\sqrt{\sum_{i=1}^{n}(x_i - \bar{x})^2}\sqrt{\sum_{i=1}^{n}(y_i - \bar{y})^2}}$$

where r is the correlation coefficient of the two variables, $\bar{X}$ and $\bar{Y}$ are the average of the two variables over the time series and n is the number of years. In addition, the t-test was used to test the significance of the correlation (Zhang et al., 2023).
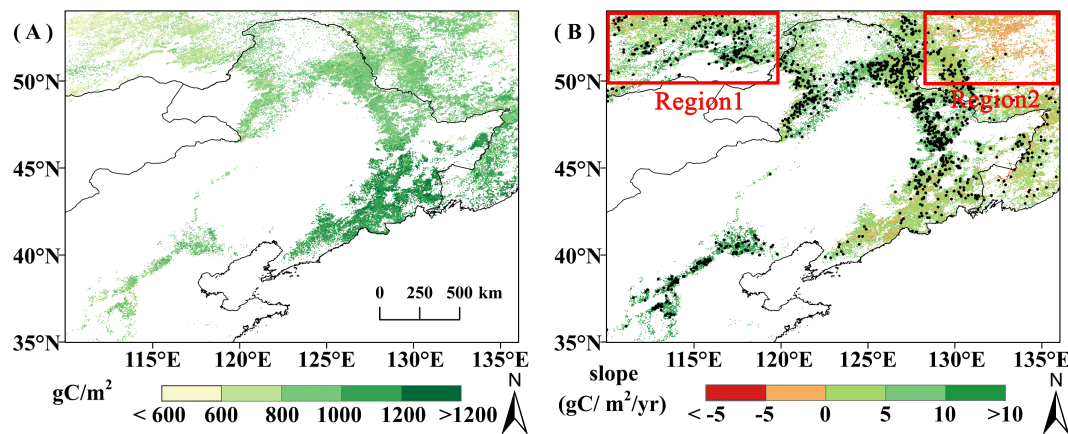
FIGURE 2
(A) Spatial distribution of average GPP$_{GS}$ from 2001 to 2020; **(B)** Spatial trend of GPP$_{GS}$ from 2001 to 2020, pixel points with dots indicate significant trends (P<0.05).
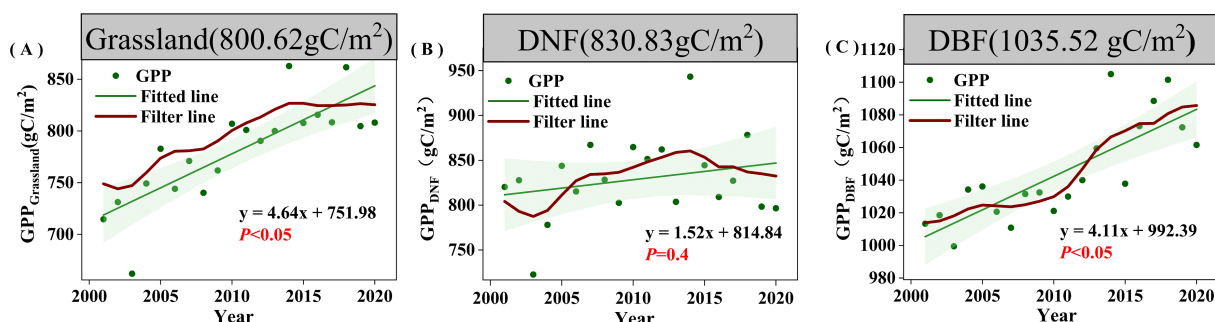

FIGURE 3
Changes in GPP$_{GS}$ for different vegetation types from 2000 to 2020.**(A)** Grassland. **(B)** DNF. **(C)** DBF. The red line represents the result of nine-point binomial filter with reflected ends; the green line represents the trend line; and the numbers in the grey boxes represent the mean GPP$_{GS}$ of the corresponding vegetation types.

3 Results

3.1 Spatiotemporal distribution and change of GPP$_{GS}$

Spatially, average GPP$_{GS}$ increased from northwest to southeast (Figure 2A). This is consistent with the spatial distribution of vegetation types and climate. Precipitation and temperature during the growing season increase from northwest to southeast, and the higher GPP$_{GS}$ areas were basically distributed in the deciduous broad-leaved forest distribution area with better temperature and moisture conditions, while the lower GPP$_{GS}$ areas were distributed in the grassland and deciduous coniferous forest distribution area with relatively poor temperature and moisture conditions.

The overall average vegetation GPP$_{GS}$ was 913.81 gC/m^2, with DBF having the highest average GPP$_{GS}$ (1035.52 gC/m^2), followed by DNF (830.83 gC/m^2), and grassland (800.62 gC/m^2) (Figure 3). The trend of GPP from 2001 to 2020 is shown in Figure 2B. The area of showing an increasing trend accounted for 85.46% of the study area, of which 33.29% increased significantly (P<0.05). The areas of DBF and grassland GPP$_{GS}$ with an increasing trend is obviously more than the area with decreasing trend: increases are seen in 88.58% of DBF area (39.54% significant) and 88.62% of grassland area (39.32% significant). The area of DNF GPP$_{GS}$ with an increasing trend (50.47%) was basically the same as the area with a decreasing trend (49.49%), but the much more of the increasing trend areas was significant (31.46% compared with 0.80%). Increases in DNF GPP$_{GS}$ are mainly located in the relatively arid northwest corner of the study area (Figure 2B, Region 1), while decreases in DNF GPP$_{GS}$ are primarily found in the relatively humid northeast corner of the study area (Figure 2B, Region 2). That is, for DNF, spatial variation in the trend is connected with background moisture conditions. The area of significant decline in grassland GPP$_{GS}$ is mainly distributed in the eastern part of the study area, and there is no obvious spatial difference in the DBF trend.

The overall trend of vegetation GPP$_{GS}$ in the study area from 2001 to 2020 shows a significant increase (4.12gC/m^2/yr, P<0.05). Grassland and DBF GPP$_{GS}$ showed significant increasing trends at

TABLE 1 Correlation coefficients (r) between GPP$_{GS}$ and phenological indicators of different vegetation types.

Region/Type	SOS	POS	EOS	LOS
Grassland	-0.40*	-0.71***	-0.05	0.39*
DBF	-0.52**	-0.42*	0.02	0.55**
DNF	-0.19	-0.43*	-0.04	0.12
Region1	-0.48**	-0.19	0.35	0.64***
Region2	-0.03	-0.41*	-0.26	-0.15

*Significant at the 0.1 level; **Significant at the 0.05 level; ***Significant at the 0.01 level. Region1 represent DNF located in the relatively arid area, Region2 represent DNF located in the relatively humid area.

similar magnitudes of 4.64gC/m^2/yr and 4.11gC/m^2/yr (P<0.05), respectively; while DNF GPP$_{GS}$ showed a non-significant increasing trend with the smallest magnitude of 1.52gC/m^2/yr (P=0.4) (Figure 3). For DNF, relatively arid Region 1 had a significant increase in GPP$_{GS}$ (6.68gC/m^2/yr, P<0.05), and relatively humid Region 2 had a non-significant decreasing trend (-0.43gC/m^2/yr, P=0.85).

As can be seen from Figure 3, DBF GPP$_{GS}$ in the study area showed a continuous increase from 2001 to 2020, while DNF and grassland GPP$_{GS}$ had a similar trends, i.e., both diverged around 2014. Among them, grassland showed a significant increasing trend before 2014, at 7.42 gC/m^2 per year (P<0.05), with growth leveling off after 2014, while DNF GPP$_{GS}$ also showed a significant upward trend before 2014, with a trend of 6.79gC/m^2 per year (P<0.05), and then showed a slight decline after 2014. Compared with the trend during 2001-2014, the increase rates of DBF, grassland, and DNF GPP$_{GS}$ were 6%, 37.44%, and 77.59% lower, respectively, than the trend during the period between 2001 and 2020.

In summary, the interannual variation in GPP$_{GS}$ of DNF and grassland diverged around 2014. In order to further understand the reasons for the different temporal change character in GPP$_{GS}$ of different vegetation types, we first examined the sensitivity and the relationship between changes in GPP$_{GS}$ and changes in phenology of different vegetation types.

3.2 GPP$_{GS}$ phenology sensitivity

The correlations between GPP$_{GS}$ and phenological indicators showed some significant relationships (Table 1). The common feature was that all vegetation types had a significant negative correlations between GPP$_{GS}$ and POS, while the overall correlation with EOS was weak and insignificant, indicating that EOS was not the main factor affecting vegetation gross primary productivity. Meanwhile, grassland and DBF showed significant negative correlations between GPP$_{GS}$ and SOS and significant positive correlations with LOS. For DNF, there was a significant negative correlation of GPP$_{GS}$ with POS in the relatively humid area (Region 2), while in the relatively arid area (Region 1) there was a significant negative correlation with SOS and a significant

positive correlation with LOS, but with no significant correlation with POS.

During 2001-2020, vegetation GPP$_{GS}$ was negatively correlated with SOS in 71.90% of the study area and with and POS in 71.80% of the study area; the correlations were statistically significant for 19.08% and 19.20% of the area, respectively. GPP$_{GS}$ was positively correlated with LOS in 66.96% of the study area (significant in 18.29%). The percentages with positive and negative correlations with EOS (47.12% and 52.88%) did not differ much, with neither direction achieving statistical significance for more than 10% of the area.

In terms of different vegetation types, unlike the significant correlation between regional mean DNF GPP$_{GS}$ and POS, the percentage of DNF area with GPP$_{GS}$ significantly correlated with any of the phenological factors was relatively small (none of them was more than 10%). Grassland GPP$_{GS}$ was more affected by POS, with 83.96% of pixels negatively correlated with POS (among which 28.22% were significantly correlated, P<0.05). DBF GPP$_{GS}$ was relatively more affected by SOS, with 77.5% of pixels negatively correlated with SOS (15.19% significant, P<0.05), which was approximately the same as that of the correlation between the regional average GPP$_{GS}$ and phenological factors (Figure 4).

According to the correlation results, SOS, POS, and LOS may be the phenological factors that cause changes in GPP$_{GS}$. In order to compare the temporal changes of phenology and GPP$_{GS}$, we use a nine-point binomial filter to smooth out year-to-year variations and show the longer-term trends. POS showed a non-significant trend of advancement in all vegetation types, with a relatively small proportion of significant pixels. SOS was significantly advanced only in the grassland area with a trend of −0.40 day yr^{-1} (P<0.1) (Figure 5), while the DBF and DNF areas showed non-significant trends. LOS showed significant lengthening trends (P<0.05) in all vegetation types, with the most substantial increase in DNF (0.63 day yr^{-1}), followed by grassland (0.55 day yr^{-1}), and the smallest increase in DBF (0.43 day yr^{-1}). This suggests that the lengthening of LOS in grassland and DBF affects GPP$_{GS}$ to some extent, and advance of SOS in grassland can enhance the growth of GPP$_{GS}$.

Further comparing the temporal change of phenological factors and GPP$_{GS}$ in each vegetation type, we found that SOS did not advance consistently in all vegetation types through 2014, but there was a pattern of advancement after 2014. This contrasts with the observed trend of significantly increasing GPP$_{GS}$ in all vegetation types through 2014 and the divergence after 2014 in DNF and grassland.

Similarly, LOS would not appear to be the dominant cause of the divergence in GPP$_{GS}$ starting in 2014. For DNF, LOS has been consistently increasing, clearly inconsistent with the pattern of decline in DNF GPP$_{GS}$ after 2014. For grassland, LOS fluctuated upward before 2016 before leveling off, failing to support the pattern of steady increase in GPP$_{GS}$ before 2014 and stagnation after 2014; the only spatially significant increase in LOS occurred in the central part of the grassland, which could not support the widespread significant increase in the trend of grassland GPP$_{GS}$.

As seen in Figure 5, the post-2014 delay and then advance in POS is clearly inconsistent with concurrent changes in GPP$_{GS}$, but the advancement of POS prior to 2014 is contributed to the rise of
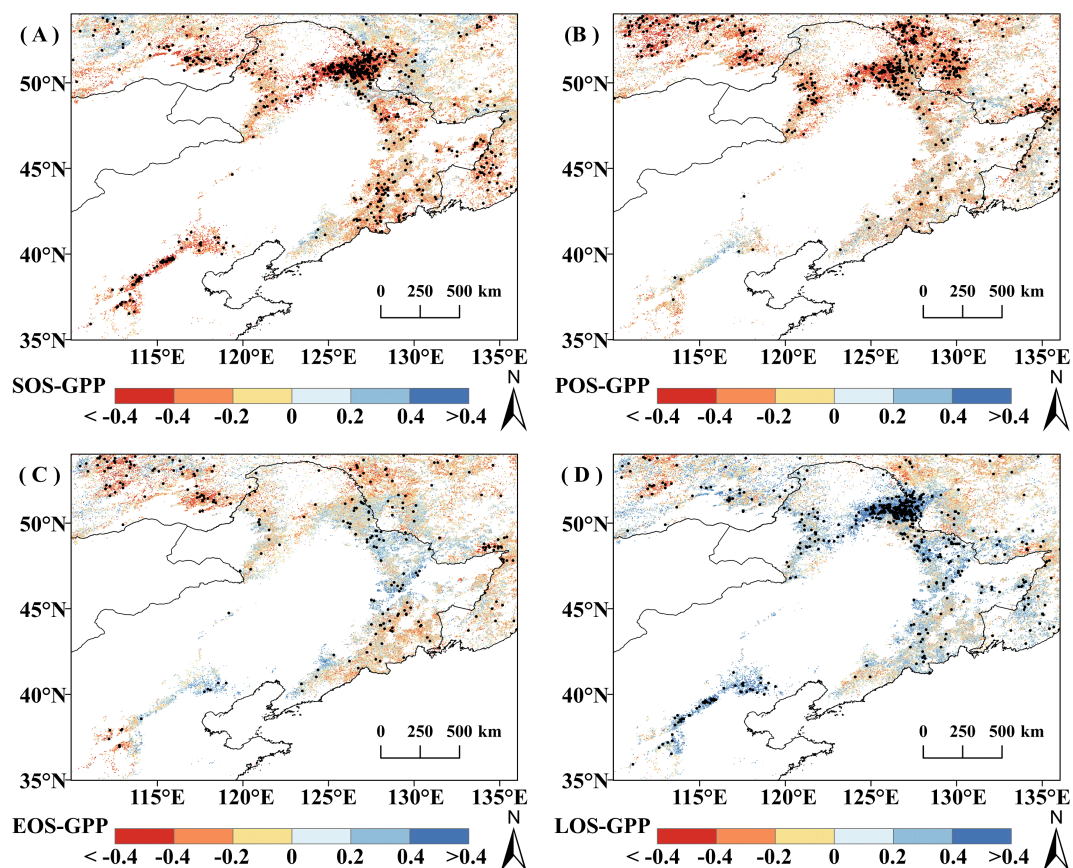
FIGURE 4
Correlation analysis between growing season cumulative productivity (GPPGS) and phenological factors from 2001 to 2020. **(A)** SOS. **(B)** POS. **(C)** EOS. **(D)** LOS , pixel points with dots indicate significant correlations (P<0.05).

GPP_{GS} in all three vegetation types. However, the proportion of pixel points where POS was significantly advanced accounted for only 9%, and the proportion of pixel points that were significantly correlated with GPP in general accounted for only 19.20%, with POS significantly correlated with GPP in only 31.94% of the pixel points that significantly increased in GPP. Thus, while POS may have played a role before 2014, but was not the main factor contributing to the change in GPP.

The above results show that, in DBF and grassland, GPP_{GS} is most strongly correlated with SOS and LOS, while across all vegetation types, the advancement of POS corresponds to increases in GPP_{GS}, especially for grassland. However, given the spatial and temporal characteristics of change of each of the phenological indicators, phenology changes are not likely to be the main drivers of the observed changes in GPP in the period of 2001-2020, so we further analyzed the relationship between climatic factors and GPP_{GS}.

3.3 GPP$_{GS}$ climate sensitivity

Among the correlations between GPP_{GS} and the growing season climatic indicators of different vegetation types (Table 2), the overall

weak and nonsignificant correlation between GPP_{GS} and T_{min} was lower than the correlation between GPP_{GS} and T_{max} for all vegetation types, indicating that T_{min} was not the main factor influencing the vegetation GPP. For DNF, the correlations of GPP_{GS} with T_{max} and PAR was both significantly positive, while the correlations with P and SM was significantly negative. Unlike DNF GPP_{GS}, DBF GPP_{GS} was significantly positively correlated with P but not significantly correlated with T_{max} and PAR. In addition, DBF and grassland GPP_{GS} were both strongly and significantly positively correlated with RH and significantly and negatively correlated with VPD. This suggests that the ability of DNF to produce organic matter is limited by thermal conditions but inhibited by excessive moisture, while grassland and DBF are limited by water conditions. In addition, DNF in the relatively humid area (Region 2) was also significantly correlated with PAR and T_{max}, and negatively correlated with SM and P, while DNF in the relatively arid area (Region 1) was not significantly correlated with climatic factors. This suggests that the DNF results are more reflective of the relatively humid area, which accounts for a greater number of pixels that of the relatively arid area.

The spatial character of correlation between GPP_{GS} and climate indicators is similar to those of the correlation between regional mean GPP_{GS} and climatic indicators (Figure 6). Overall, in 78.82% of the
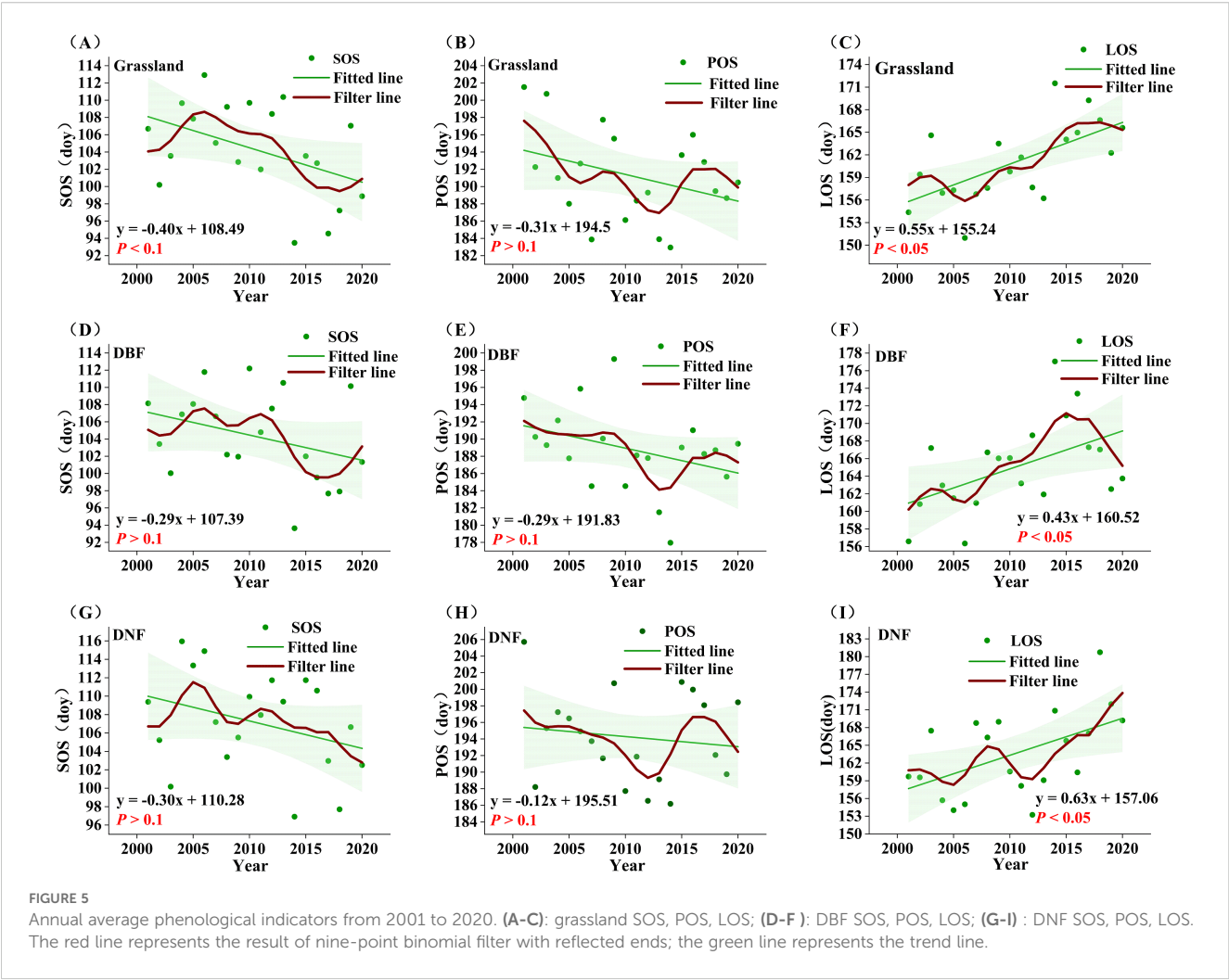
FIGURE 5
Annual average phenological indicators from 2001 to 2020. **(A-C)**: grassland SOS, POS, LOS; **(D-F)**: DBF SOS, POS, LOS; **(G-I)** : DNF SOS, POS, LOS.
The red line represents the result of nine-point binomial filter with reflected ends; the green line represents the trend line.

TABLE 2   Correlation coefficients (r) between GPP_{GS} and growing season climate indicators of different vegetation types.

Region/Type	T_{max}	T_{min}	P	PAR	RH	VPD	SM
Grassland	0.31	0.14	-0.13	0.24	0.62***	-0.41*	-0.12
DBF	0.30	0.24	0.42*	-0.17	0.63***	-0.46**	0.27
DNF	0.70***	0.01	-0.47**	0.69***	-0.07	0.37	-0.75***
Region1	0.27	0.19	0.22	0.15	0.31	-0.03	-0.06
Region2	0.69***	0.01	-0.57***	0.77***	-0.10	0.38*	-0.65***

*Significant at the 0.1 level; **Significant at the 0.05 level; ***Significant at the 0.01 level. Region1 represent DNF located in the relatively arid area, Region2 represent DNF located in the relatively humid area.

study area, vegetation GPP_{GS} was positively correlated with RH (of which 39.56% is significant, $P<0.05$). Vegetation GPP_{GS} was negatively correlated with PAR and T_{max} in the most of the study area, with 75.32% (26.27% significant) and 75.26% (20.14% significant) respectively. Vegetation GPP_{GS} was negatively correlated with VPD in 69.42% of the area (29.98% significant, $P<0.05$). The correlations between vegetation GPP_{GS} and SM or T_{min} did not reach a significant level over a large area, and the percentage of significantly correlated pixels did not exceed 15% ($P<0.05$).

In terms of different vegetation types, DBF and grassland GPP_{GS} were more affected by RH and VPD. The proportion of DBF pixels positively correlated with RH was 72.74% (34.46% significant, $P<0.05$) and those negatively correlated with VPD was 63.36% (33.79% significant, $P<0.05$), while the proportion of grassland GPP_{GS} pixels positively correlated with RH was 91% (47.05% significant, $P<0.05$) and those negatively correlated with VPD was 84.87% (39.19% is significant, $P<0.05$). DNF GPP_{GS} was most greatly affected by T_{max} and PAR, with 93.26% of pixels
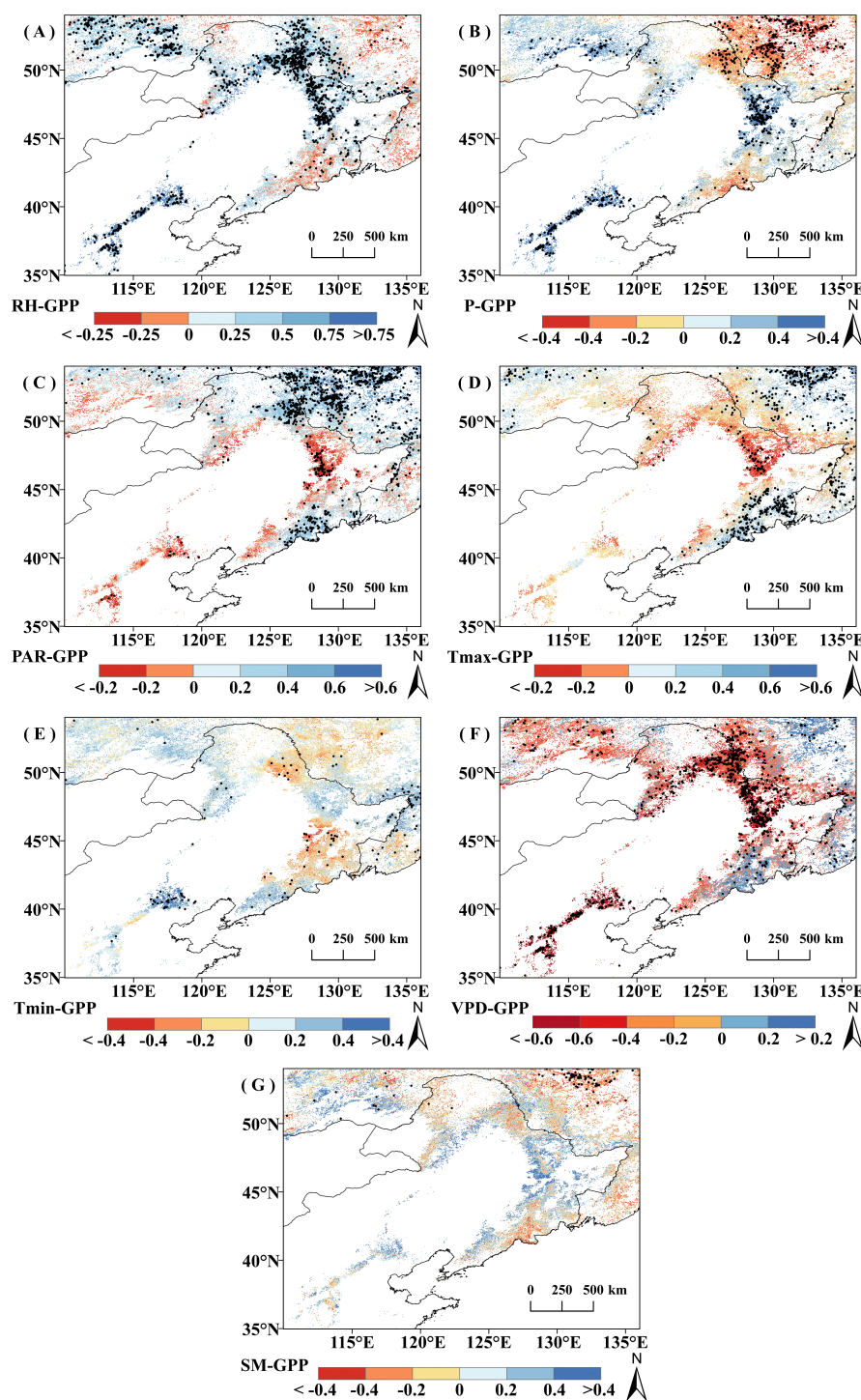
FIGURE 6
Correlation coefficient (r) between growing season cumulative productivity (GPP$_{GS}$) and climatic factors from 2001 to 2020; pixel points with dots indicate significant correlations (P<0.05). **(A)** RH. **(B)** P. **(C)** PAR. **(D)** Tmax. **(E)** T min. **(F)** VPD. **(G)** SM.

positively correlated with T$_{max}$ (62.73% is significant, *P*<0.05) and 90.71% with PAR (73.78% significant, *P*<0.05).

It is worth noting that there was obvious spatial variability in the effects of P on GPP$_{GS}$ in grassland and DNF, with a largely positive response to P distributed mainly in the relatively arid region and negative correlations mainly distributed in the humid

region adjacent to the sea. Positive and negative correlations offset each other, resulting in a nonsignificant correlation of GPP$_{GS}$ with P for grasslands and a significant negative correlation for DNF, which is concentrated in the relatively wet zone, Region 2. Similarly, DNF GPP$_{GS}$ was significantly positively correlated with current year RH mainly in the northwestern part of the study area (Region 1), and
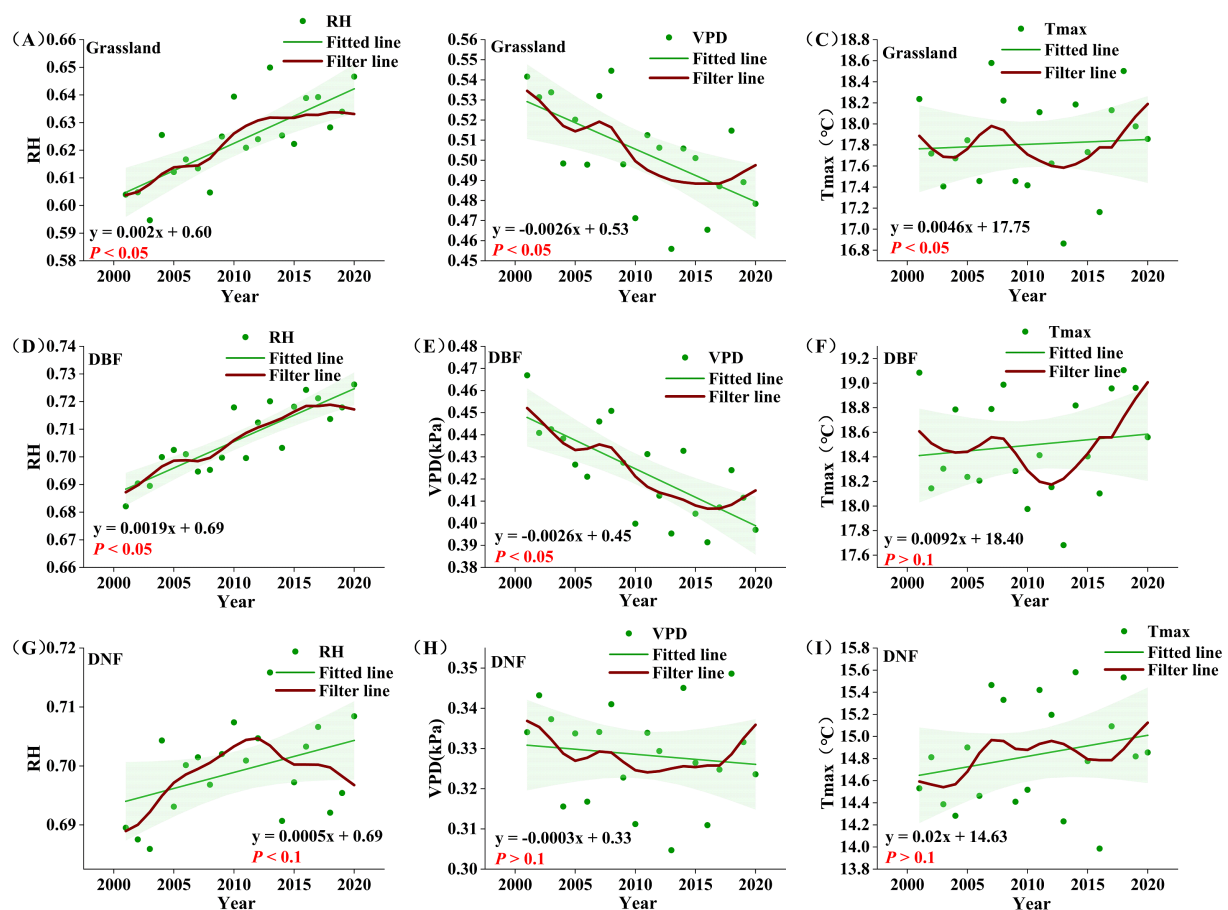
FIGURE 7
Growing season average climate factors for different vegetation types from 2001 to 2020. **(A-C)** : grassland RH, VPD, Tmax; **(D-F)** : DBF RH, VPD, Tmax; **(G-I)** : DNF RH, VPD, Tmax. The red line represents the result of nine-point binomial filter with reflected ends; the green line is the trend line.

negatively correlated with current year RH mainly in the relatively wet region in the northeastern part of the study area (Region 2).

According to the correlation results, RH, VPD, and T_{max} are most likely the climate factors that lead to the rise of GPP_{GS} before 2014 and the divergence after 2014. Comparing the temporal change characteristics of climate and GPP_{GS}, apart from the overall trend, similarly, a 9-point binomial filtering method was used to reveal the longer-term change. As shown in Figure 7, T_{max} showed a nonsignificant increasing trend in all three vegetation types (P>0.1); VPD showed a significant decreasing trend in grassland and DBF areas (P< 0.1), while RH showed a significant increasing trend in all vegetation types (P<0.1). In DNF areas, there was a significant increasing trend in RH in the relatively arid Region 1 (P<0.1), but a non-significant decreasing trend in the relatively wet Region 2 (P >0.1).

Comparing the temporal change in climate factors and GPP_{GS} for each vegetation type, we see that T_{max} was consistent with the change in GPP_{GS} of all vegetation types before 2008. After 2008, T_{max} experienced a decrease and then an increase, at odds with steady increase in GPP_{GS} before 2014 and divergence after 2014. Spatially, the significant decreasing trend of T_{max} was mainly distributed in the northern part of the DBF distribution; the significant increasing trend of GPP_{GS} is also mainly distributed in

the northern part of DBF. As GPP_{GS} is positively correlated with T_{max}, changes in T_{max} could not be the cause.

For both grassland and DBF, VPD shifted from a sustained decline to an obvious increase around 2016, which clearly does not correspond with the temporal change in GPP_{GS}. For DNF, there was a double peak in the interannual variability of VPD and neither was in 2014. Thus, VPD also could not be the cause of the transition of GPP_{GS} around 2014.

On the other hand, the temporal changes of RH were consistent with the temporal change in GPP_{GS} for all vegetation type. Grassland RH showed an obvious change point around in 2014, with a significant increasing trend before 2014 (P<0.05); the growth rate then declined and flattened after 2014, which is compatible with the main interannual change characteristics of grassland GPP_{GS}. DBF RH basically maintained an upward trend, basically tracking the interannual change characteristics of DBF GPP_{GS}, while DNF RH, on the other hand, generally matched the change pattern of DNF GPP_{GS}, but with a lag of around one year. We note that the portion of the study area with the significant increase in RH generally overlapped with the region of significant increase in GPP (Figures 2, 6).

In order to see whether there is a lag effect of climate factors on GPP_{GS}, we calculated the correlation between GPP_{GS} and the

TABLE 3 Correlation coefficients (r) between GPP$_{GS}$ and climate indicators of the previous year's growing season.

Region/Type	T$_{max}$	T$_{min}$	P	PAR	RH	VPD	SM
Grassland	-0.35	-0.19	0.54**	-0.44*	0.73***	-0.72***	0.33
DBF	-0.04	0.27	0.54**	-0.48**	0.81***	-0.70***	0.27
DNF	-0.22	-0.17	0.27	-0.08	0.75***	-0.66***	-0.15
Region1	-0.25	0.1	0.45*	-0.35	0.39*	-0.33	-0.12
Region2	-0.19	-0.13	0.12	0.01	0.69***	-0.65***	-0.06

*Significant at the 0.1 level; **Significant at the 0.05 level; ***Significant at the 0.01 level. Region1 represent DNF located in the relatively arid area, Region2 represent DNF located in the relatively humid area.

TABLE 4 Percentage of pixels with positive correlation between GPP$_{GS}$ and Relative Humidity (RH) of previous year and current year for different vegetation types.

vegetation type / climatic factor	DNF	DBF	Grassland
Previous year	88.29%(29.76%)	85.92%(34.82%)	94.05%(41.71%)
Current year	49.67%(10.13%)	72.74%(34.46%)	91.00%(47.05%)

Percentage with significant correlations are shown in parentheses (*P*<0.05).

previous year's growing season climate indicators for the three vegetation types (Table 3). We found that the temperature of the previous year was not significantly correlated with the GPP$_{GS}$. However, DBF and grassland GPP$_{GS}$ were significantly positively correlated with the precipitation of the previous year and were significantly negatively correlated with the PAR of the previous year —more so than with the precipitation or PAR of the current year. The GPP$_{GS}$ of all three vegetation types were significantly positively correlated with the RH and VPD of the previous year, again with higher correlations than with the RH and VPD of the current year. For DNF, GPP$_{GS}$ in the relatively humid area (Region 2) also maintained significant relationships with previous year's RH, VPD, and SM, while in the relatively arid area (Region 1) GPP$_{GS}$ was only significantly positively correlated with previous year's precipitation and, to a much lesser extent than in Region 2, RH. This suggests that the variation of GPP$_{GS}$ in the study area is strongly influenced by the atmospheric moisture conditions of the previous year, while drier air in the previous year has an inhibitory effect on GPP$_{GS}$. Grassland and DBF GPP$_{GS}$ are also affected by the legacy of precipitation and solar radiation in the previous year.

Comparing the possible influences of RH and VPD on GPP, we note that the temporal and spatial trends of VPD differ from those of GPP, whereas both the temporal and spatial changes in RH correspond with GPP$_{GS}$ for each of the vegetation types. In addition, the correlations between space and regional average mean GPP$_{GS}$ and the climate indicators were highly consistent, and RH in the previous year general had a stronger effect on GPP$_{GS}$ than the current year for all three vegetation types. These is more obvious for DNF: DNF GPP$_{GS}$ is not significantly correlated with the current year's RH; however, it is strongly significantly correlated with the RH of the previous year. Spatially, the percentage of pixel points significantly correlated with the RH of the previous year is 19.63 percentage higher than that of the current year (Tables 2-4). Therefore, we conclude that the dominant

factor causing the stagnation of GPP$_{GS}$ in grassland and DNF after 2014 was RH, and the effect of RH on vegetation GPP$_{GS}$ had a lagged effect. Thus, based on the spatial correspondence, temporal synchrony, and significance of the change, we argue that the change in GPP$_{GS}$ in the study area during these two decades was mainly driven by RH, particularly the previous year's RH.

In addition, in order to determine whether the legacy effect of RH comes from the whole growing season or a specific period, we calculated the correlation between average RH in different periods of the previous year's growing season (July-October, August-October, and September-October) and GPP for each vegetation type. We found that the strongest correlation between the GPP and the RH for these three periods was August-October (DNF: 0.60; DBF: 0.80; grassland: 0.72), but still slightly lower than the correlation between GPP and previous year's entire growing season RH. This shows that the legacy effect of RH comes from the entire growing season, not just the last few months. To further validate the optimal lag period, we performed a cross-correlation function (CCF) analysis test and found results slightly lower than those for pairwise correlations, but the results were consistent with DNF, DBF, and grassland GPP$_{GS}$ all having the strongest correlations with the previous year's RH (0.72, 0.73, 0.67) and still stronger than with the current year's RH (-0.07, 0.63, 0.62).

4 Discussion

4.1 Characteristics of GPP$_{GS}$ changes in different vegetation types and their response to climate

Moisture and temperature and their synergistic effects are the main factors affecting vegetation growth and distribution (Sun et al.,

2002). Overall, the spatial variation of vegetation GPP was highly consistent with the spatial variation of average hydrothermal conditions. The overall multiyear average GPP_{GS} in the study area showed a gradual increase from northwest to southeast with the increase of temperatures and moisture conditions, and the area with increasing GPP (85.46%) was much higher than that with decreasing GPP, corresponding with the overall trend toward increasing carbon sequestration capacity in China in recent years (Huang et al., 2022; Wu et al., 2023).

The mean GPP_{GS} of different vegetation types showed obvious differences: DBF displayed the largest GPP_{GS}, mainly distributed in the temperate humid southeastern part of the study area; DNF GPP_{GS} was lower than DBF and mainly distributed in the colder northern part of the study area; and grassland GPP_{GS}, lowest among the three vegetation types, was mainly distributed in temperate western part of study area. Previous studies have confirmed that these differences are closely related to the background climatic conditions, and the physiological structure of the vegetation (Liu et al., 2020a; Gui et al., 2021). On the one hand, the broad-leaved forests, with larger leaf area, have a strong carbon sink ability (Zhang et al., 2020; Ali et al., 2023); on the other hand, forests with a higher canopy structure and a deeper distribution of the root system are obviously more advantageous than the grasslands in terms of their carbon sequestration capacity (Ye et al., 2021; Lu and Yan, 2023).

We mainly considered climate change during the plant growing season when analyzing the effect of climate on vegetation GPP. The results showed that the average GPP_{GS} of different vegetation types vary in their sensitivity to climate indicators, which was consistent with the results of a previous study on the relationship between productivity and climate factors for grassland, shrublands, forests, etc (Xu et al., 2024). Our results further confirm that tree leaf form affects the sensitivity of GPP to climate. We found that DNF GPP is significantly correlated with current year T_{max} and PAR. This was explained by the facts that, on the one hand, because the DNF was distributed in the cold temperate climatic zone, PAR was significantly lower than that of other vegetation type distribution, so carbon absorption is more limited by light; on the other hand, conifer leaf area is relatively small and mainly receives scattered light, resulting in a large effect of light on its assimilation process (Chen et al., 2024a).

Grassland and DBF GPP_{GS} are mainly affected by changes in RH, which integrates the water and heat conditions of a region (Niu et al., 2020). RH has been found to be a dominant factor influencing the spatial differentiation of biomass in vegetation (Dragoni et al., 2011). We suggest that the role of RH in determining the changes in vegetation productivity can be explained in the following ways: When RH is high, atmospheric water vapor is more likely to condense into water droplets and fall on the ground to replenish soil moisture, which in turn reduces evaporation loss of water, reduces the need to transport water from the soil through the roots, and slows down the transpiration process, which effectively reduces the dissipation of moisture from the vegetation, keeps the vegetation in a better water status, and promotes photosynthesis (Baldocchi et al., 2018). When RH is low, it contributes to an increase in transpiration rate, inducing rapid closure of leaf stomata to reduce excessive water loss, however, this also results in the inaccessibility of carbon dioxide, which depletes carbohydrate reserves and leads to carbohydrate starvation at the tissue level, thus inhibiting GPP growth (Buckley, 2019; Hsu et al., 2021; Song et al., 2021). The fact that air moisture emerges as the dominant factor for recent GPP change implies that relative importance in water conditions will increase under conditions of global warming.

Unlike the results of previous studies that found that changes in grassland biomass were more sensitive to precipitation than to temperature (Beer et al., 2010), the present study found that grassland GPP_{GS} was not significantly correlated with precipitation or temperature, which may be due to the distribution of grassland in the study area. Grasslands selected for the present study were mainly located in the northern part of the study area where precipitation varied considerably; this led to a polarization of the correlation between grassland GPP_{GS} and precipitation, with the proportion of image points with positive and negative significant correlations between GPP_{GS} and precipitation accounting for 8.85% and 9.50%, respectively (Figure 6). These nearly equal proportions neutralized the relationship of grassland GPP_{GS} with precipitation, which ultimately led to a nonsignificant correlation.

In contrast to grassland GPP_{GS}, both forest vegetation types were regulated by precipitation, but they showed opposite significant correlations: DNF is significantly negatively correlated with precipitation while DBF was significantly positively correlated with precipitation. This may be due to the fact that the distribution of DNF in the study area is mainly in the eastern coastal region of Russia, which is subject to the influence of the southeast monsoon from the sea in summer and receives more abundant precipitation. Further more, deciduous-coniferous forests are inherently resistant to cold and drought and do not have a high water demand (Jia et al., 2023). Therefore, increased precipitation inhibited the accumulation of GPP in relative humid DNF distribution.

The same is true for soil moisture. The dominant DNF species in the study area, the Dahurian larch (*Larix gmelinii*), is adapted to survive in well-drained soils (Rehfeldt and Jaquish, 2010). As an abundance of precipitation raises soil moisture and can lead to water-filled soil pores, root hypoxia, the inhibition of respiration and metabolic activity of aerobic microorganisms in tree roots, and a reduction of water and nutrient uptake efficiency, thus limiting photosynthesis (Costa et al., 2023; Peng et al., 2024). This is consistent with the significant negative correlation between GPP and SM in the relatively humid DNF distribution. In addition, the effect of precipitation on vegetation GPP is generally less than that of relative humidity, because precipitation is not directly converted into available water for vegetation, but indirectly regulate the carbon sequestration capacity of vegetation through affects soil and atmospheric humidity (Driesen et al., 2020). For vegetation growing in low-latitude south China, prior research found that relative humidity strongly affects GPP, surpassing the effects of precipitation and soil moisture (Xu et al., 2024), consistent with our results. However, that study observed lag effects in net solar radiation and surface temperature, while our results confirm that

RH had the strongest legacy effects on vegetation in middle to high latitude vegetation.

It is noteworthy that the GPP_{GS} of all vegetation types is affected more by the RH of the previous year than by the RH of the current year, DNF most of all. This indicates that the degree of atmospheric drought in the previous year would largely affect carbon absorption in the current year. This is related with to legacy effect of changes in the moisture available at various points in the vegetation life cycle: One possibility is that changes in air humidity in the previous year may alter plant roots and leaves development and density (Liu et al., 2021a; Hu et al., 2025), which in turn affects vegetation carbon absorption in the coming year. This effect is common in arid to semi-moist climate ecosystems: the strong legacy effect of previous year's precipitation on NPP leads to improved moisture conditions, enhancing root and canopy development, which is then helpful for the next year's carbon absorption (Sala et al., 2012).

In addition, trade-offs between immediate plant growth and long-term survival may also be considered (Chuine, 2010; Yuan et al., 2019). In terms of long-term climate adaptation, photosynthetic products from the growing season of the previous year may not be used for immediate growth, but, rather, stored as non-structural carbohydrates in the root system, branches, or seeds (Meng et al., 2023a), which are mainly used to cope with climatic stress and for initiating growth early in the following year. Thus, carbon storage for survival is prioritized over immediate growth to reduce the risk of mortality (Olano et al., 2023), it seems that improvement in hydro-thermal condition can reduce the survival cost which is benefit for plant growth.

Our results highlight how GPP responses to climate vary considerably among different vegetation types and support prior findings that time-lag effects are quite important for better predicting and evaluating changes in vegetation dynamics that may accompany global warming (Wu et al., 2015).

4.2 Characteristics of GPP_{GS} response to phenology for different vegetation types

Among the relationships between phenology and GPP_{GS}, the significant negative correlation between vegetation GPP_{GS} and POS—strongest in grasslands—is most notable. This relationship can be explained in two ways. First, earlier POS promotes vegetation carbon assimilation throughout the growing season, which ultimately leads to an increase in productivity (Wang and Wu, 2019). Second, plants experiencing earlier POS can take advantage of favorable spring climatic conditions (Gonsamo et al., 2018; Wang and Wu, 2019), enhance photosynthesis, and mitigate to some extent the potential damage to plant growth caused by high summer temperatures and drought (Liu et al., 2021b), prolonging the growing season and ultimately increasing vegetation productivity. Grasslands have more rapid growth rates and resource acquisition capacity compared to forests (Yan et al., 2025), which means that more of their productivity is concentrated in the peak growth period when temperature and moisture conditions are favorable. The peak growth period inherently represents the time of maximum

availability of resources for vegetation growth (Shen et al., 2024a); favorable climatic conditions contribute to the fact that the period in which the POS occurs accounts for more than half of the year's productivity (Yang et al., 2024). Furthermore, the shorter growth period of herbaceous plants also accentuates the role of changes in the summer peak growth period in influencing productivity (Zhou, 2020).

Overall, the relationship between GPP_{GS} changes and phenological responses was not as strong as that with climatic factors during 2001-2020. On the one hand, because the 2001–2020 POS showed a non-significant trend of advancement in all vegetation types, its contribution to the GPP change was necessarily limited. On the other hand, because the study area is located in the middle to high latitudes of the Northern Hemisphere, which is quite sensitive to climate change, GPP is mainly affected by the efficiency of photosynthesis, which is directly dependent on climatic factors such as temperature, precipitation, and so on (Du et al., 2022; Wang et al., 2022b). While phenological changes are often attributed to the corresponding climate change effects (Coomes et al., 2014), their independent effects may be masked by concurrent climate changes. In addition, it has been found that for many northern ecosystems, the benefits of warmer springs on growing-season ecosystem productivity are effectively compensated by the accumulation of seasonal water deficits (Buermann et al., 2018), i.e., as the phenology advances, GPP is likely to become more strongly influenced by moisture conditions.

Our results emphasize that the capacity of middle to high latitude Northeast Asia vegetation to act as a future carbon sink depends critically on the air moisture. The contribution of water deficits to GPP variation suggests that carbon uptake in northern middle to high latitude ecosystems may be more determined by moisture conditions. This can help provide an important basis for ecosystem management or carbon sink policies under future climate scenarios. Ecosystem managers may need to focus on maintaining soil moisture through enhanced water retention strategies, such as improving organic matter content and implementing water-conserving land use practices. Management decisions should consider not just current conditions but also how previous years' climate patterns will influence ecosystem responses. This may require developing early warning systems and adaptive management protocols that can respond to multi-year climate patterns.

5 Conclusions

In this study, we analyzed the relationships between vegetation growing season cumulative gross primary productivity (GPP_{GS}) and vegetation phenology and climatic factors in the mid- to high-latitude regions of East Asia to assess the dominant factors influencing the changes in GPP_{GS} of different vegetation types from 2001 to 2020. We found:

1. Among the phenology factors, the advancement of POS has a positive effect on GPP_{GS} of all three vegetation types, with grassland being the most affected by POS due to its strong

opportunist characteristics; the advancement of SOS also has a positive effect on GPP_{GS} of grasslands and DBF, while DNF GPP_{GS} was less responsive to phenology variation.

2. Relative humidity in the previous year had a stronger positive effect than the current year on changes in the GPP_{GS} of all three vegetation types, especially that of DNF in humid areas. Soil moisture of current year has negative effect on the vegetation productivity of DNF, and T_{max} and PAR in the current year have positive effect on the vegetation productivity of DNF. For both grasslands and DNF, the vegetation in drier regions had a higher sensitivity to precipitation.

3. Over these two decades, the overall trend of vegetation GPP_{GS} in the middle and high latitude regions of East Asia showed a significant increase, with obvious differences for different vegetation types. Before 2014, all three vegetation types showed significant increasing trends. Since 2014, DBF GPP_{GS} maintained its increase trend, while the growth rate of grassland GPP_{GS} flattened and that of DNF slightly decreased. RH dominate the changes of GPP_{GS} for all three vegetation types, indicating that changes in vegetation productivity were more influenced by atmospheric moisture conditions in this study area during recent decades.

In conclusion, this paper summarizes the effects of climatic and phenological changes on vegetation GPP_{GS}, highlighting the significant legacy effects of changes in RH of the previous year on GPP and pointing to the importance of changes in RH accompanying global warming. In addition, we find that DNF GPP_{GS} differs from the other vegetation types in that it is less affected by phenology changes, affected more by lower temperatures and excess moisture. At the same time, both grasslands and coniferous forests are also strongly influenced by background climate conditions. Therefore, we need to pay attention to the effects of changing climate and phenology on different vegetation types. These findings provide new insights into the complex relationships among phenology, climate and vegetation productivity.

Data availability statement

The original contributions presented in the study are included in the article/supplementary material. Further inquiries can be directed to the corresponding author.

Author contributions

Funding

Conflict of interest

Author XG was employed by the company Changzhou Architectural Research Institute Group Co., Ltd.

The remaining authors declare that the research was conducted in the absence of any commercial or financial relationships that could be constructed as a potential conflict of interest.

Generative AI statement

The author(s) declare that no Generative AI was used in the creation of this manuscript.

Publisher's note

All claims expressed in this article are solely those of the authors and do not necessarily represent those of their affiliated organizations, or those of the publisher, the editors and the reviewers. Any product that may be evaluated in this article, or claim that may be made by its manufacturer, is not guaranteed or endorsed by the publisher.

References

Abbas, S., Nichol, J. E., and Wong, M. S. (2021). Trends in vegetation productivity related to climate change in China's Pearl River Delta. *PLoS One* 16, e0245467. doi: 10.1371/journal.pone.0245467

Ahlström, A., Raupach, M. R., Schurgers, G., Smith, B., Arneth, A., Jung, M., et al. (2015). The dominant role of semi-arid ecosystems in the trend and variability of the land CO_2 sink. *Science* 348, 895–899. doi: 10.1126/science.aaa1668

Ali, S., Khan, S. M., Ahmad, Z., Abdullah, A., Kazi, N., Nawaz, I., et al. (2023). Relative humidity, soil phosphorus, and stand structure diversity determine aboveground biomass along the elevation gradient in various forest ecosystems of Pakistan. *Sustainability* 15, 7523. doi: 10.3390/su15097523

Anav, A., Friedlingstein, P., Beer, C., Ciais, P., Harper, A., Jones, C., et al. (2015). Spatiotemporal patterns of terrestrial gross primary production: A review. *Rev. Geophysics* 53, 785–818. doi: 10.1002/2015RG000483

Baldocchi, D., Chu, H., and Reichstein, M. (2018). Inter-annual variability of net and gross ecosystem carbon fluxes: A review. *Agric. For. Meteorology* 249, 520–533. doi: 10.1016/j.agrformet.2017.05.015

Beer, C., Reichstein, M., Tomelleri, E., Ciais, P., Jung, M., Carvalhais, N., et al. (2010). Terrestrial gross carbon dioxide uptake: global distribution and covariation with climate. *Science* 329, 834–838. doi: 10.1126/science.1184984

Buckley, T. N. (2019). How do stomata respond to water status? *New Phytol.* 224, 21–36. doi: 10.1111/nph.15899

Buermann, W., Forkel, M., O'Sullivan, M., Sitch, S., Friedlingstein, P., Haverd, V., et al. (2018). Widespread seasonal compensation effects of spring warming on northern plant productivity. *Nature* 562, 110–114. doi: 10.1038/s41586-018-0555-7

Campbell, J. E., Berry, J. A., Seibt, U., Smith, S. J., Montzka, S. A., Launois, T., et al. (2017). Large historical growth in global terrestrial gross primary production. *Nature* 544, 84–87. doi: 10.1038/nature22030

Chen, M., Henderson, M., Liu, B., Zhou, W., Ma, R., Huang, W., et al. (2024b). Winter climate change mediates the sensitivity of vegetation leaf-out to spring warming in high latitudes in China. *Front. Plant Sci.* 15. doi: 10.3389/fpls.2024.1476576

Chen, A., Huang, L., Liu, Q., and Piao, S. (2021). Optimal temperature of vegetation productivity and its linkage with climate and elevation on the Tibetan Plateau. *Global Change Biol.* 27, 1942–1951. doi: 10.1111/gcb.15542

Chen, S., Sui, L., Liu, L., and Liu, X. (2022). Effect of the partitioning of diffuse and direct APAR on GPP estimation. *Remote Sens.* 14, 57. doi: 10.3390/rs14010057

Chen, F., Yang, X., Yu, Q., and Han, B. (2024a). Quantifying the effects of diffuse photosynthetically active radiation on water use efficiency in different ecosystems. *Agric. For. Meteorology* 356, 110191. doi: 10.1016/j.agrformet.2024.110191

Chuine, I. (2010). Why does phenology drive species distribution? *Philos. Trans. R. Soc. B: Biol. Sci.* 365, 3149–3160. doi: 10.1098/rstb.2010.0142

Coomes, D. A., Flores, O., Holdaway, R., Jucker, T., Lines, E. R., and Vanderwel, M. C. (2014). Wood production response to climate change will depend critically on forest composition and structure. *Global Change Biol.* 20, 3632–3645. doi: 10.1111/gcb.12622

Costa, F. R. C., Schietti, J., Stark, S. C., and Smith, M. N. (2023). The other side of tropical forest drought: do shallow water table regions of Amazonia act as large-scale hydrological refugia from drought? *New Phytol.* 237, 714–733. doi: 10.1111/nph.17914

Dang, C., Shao, Z., Huang, X., Zhuang, Q., Cheng, G., and Qian, J. (2023). Climate warming-induced phenology changes dominate vegetation productivity in Northern Hemisphere ecosystems. *Ecol. Indic.* 151, 110326. doi: 10.1016/j.ecolind.2023.110326

Dragoni, D., Schmid, H.p., Wayson, C.a., Potter, H., Grimmond, C., and Randolph, J.c. (2011). Evidence of increased net ecosystem productivity associated with a longer vegetated season in a deciduous forest in south-central Indiana, USA. *Global Change Biol.* 17, 886–897. doi: 10.1111/j.1365-2486.2010.02281.x

Driesen, E., Van den Ende, W., De Proft, M., and Saeys, W. (2020). Influence of environmental factors light, CO2, temperature, and relative humidity on stomatal opening and development: A review. *Agronomy* 10, 1975. doi: 10.3390/agronomy10121975

Du, Z., Liu, X., Wu, Z., Zhang, H., and Zhao, J. (2022). Responses of forest net primary productivity to climatic factors in China during 1982–2015. *Plants* 11, 2932. doi: 10.3390/plants11212932

Fu, G., Shen, Z.-X., and Zhang, X.-Z. (2018). Increased precipitation has stronger effects on plant production of an alpine meadow than does experimental warming in the Northern Tibetan Plateau. *Agric. For. Meteorology* 249, 11–21. doi: 10.1016/j.agrformet.2017.11.017

Gonsamo, A., Chen, J. M., and Ooi, Y. W. (2018). Peak season plant activity shift towards spring is reflected by increasing carbon uptake by extratropical ecosystems. *Global Change Biol.* 24, 2117–2128. doi: 10.1111/gcb.14001

Green, J. K., Seneviratne, S. I., Berg, A. M., Findell, K. L., Hagemann, S., Lawrence, D. M., et al. (2019). Large influence of soil moisture on long-term terrestrial carbon uptake. *Nature* 565, 476–479. doi: 10.1038/s41586-018-0848-x

Gui, X., Wang, L., Su, X., Yi, X., Chen, X., Yao, R., et al. (2021). Environmental factors modulate the diffuse fertilization effect on gross primary productivity across Chinese ecosystems. *Sci. Total Environ.* 793, 148443. doi: 10.1016/j.scitotenv.2021.148443

Hatfield, J. L., and Dold, C. (2019). Water-use efficiency: advances and challenges in a changing climate. *Front. Plant Sci.* 10. doi: 10.3389/fpls.2019.00103

Held, I., and Soden, B. (2000). Water vapor feedback and global warming. *Annu. Rev. Energy Environ. - Annu. Rev. ENERG Environ.* 25, 441–475. doi: 10.1146/annurev.energy.25.1.441

Hilty, J., Muller, B., Pantin, F., and Leuzinger, S. (2021). Plant growth: the what, the how, and the why. *New Phytol.* 232, 25–41. doi: 10.1111/nph.17610

Hsu, P.-K., Takahashi, Y., Merilo, E., Costa, A., Zhang, L., Kernig, K., et al. (2021). Raf-like kinases and receptor-like (pseudo)kinase GHR1 are required for stomatal vapor pressure difference response. *Proc. Natl. Acad. Sci.* 118, e2107280118. doi: 10.1073/pnas.2107280118

Hu, L., Fan, W., Ren, H., Liu, S., Cui, Y., and Zhao, P. (2018). Spatiotemporal dynamics in vegetation GPP over the great Khingan mountains using GLASS products from 1982 to 2015. *Remote Sens.* 10, 488. doi: 10.3390/rs10030488

Hu, L., Fan, W., Yuan, W., Ren, H., and Cui, Y. (2021). Spatiotemporal variation of vegetation productivity and its feedback to climate change in northeast China over the last 30 years. *Remote Sens.* 13, 951. doi: 10.3390/rs13050951

Hu, H., Liu, X., He, Y., Feng, J., Xu, Y., and Jing, J. (2025). Legacy effects of precipitation change: Theories, dynamics, and applications. *J. Environ. Manage.* 373, 123729. doi: 10.1016/j.jenvman.2024.123729

Huang, Y., Sun, W., Qin, Z., Zhang, W., Yu, Y., Li, T., et al. (2022). The role of China's terrestrial carbon sequestration 2010–2060 in offsetting energy-related CO2 emissions. *Natl. Sci. Rev.* 9, 1–14. doi: 10.1093/nsr/nwac057

Ichii, K., Hashimoto, H., Nemani, R., and White, M. (2005). Modeling the interannual variability and trends in gross and net primary productivity of tropical forests from 1982 to 1999. *Global Planetary Change* 48, 274–286. doi: 10.1016/j.gloplacha.2005.02.005

IPCC (2014). "Climate change 2014: synthesis report," in *Contribution of Working Groups I, II and III to the Fifth Assessment Report of the Intergovernmental Panel on Climate Change*. Eds. R. K. Pachauri and L. A. Meyer (IPCC, Geneva, Switzerland), 151 pp. Core Writing.

Jeong, S.-J., Ho, C.-H., Gim, H.-J., and Brown, M.e. (2011). Phenology shifts at start vs. end of growing season in temperate vegetation over the Northern Hemisphere for the period 1982–2008. *Global Change Biol.* 17, 2385–2399. doi: 10.1111/j.1365-2486.2011.02397.x

Jia, Z., Lei, R., Liu, Y., Liu, P., Wang, Z., Chang, Y., et al. (2023). Spatial–temporal variations and the driving factors of vegetation coverage in the loess hilly and gully region of China. *Forests* 14, 1238. doi: 10.3390/f14061238

Jonsson, P., and Eklundh, L. (2002). Seasonality extraction by function fitting to time-series of satellite sensor data. *IEEE Trans. Geosci. Remote Sens.* 40, 1824–1832. doi: 10.1109/TGRS.2002.802519

Li, F., Xiao, J., Chen, J., Ballantyne, A., Jin, K., Li, B., et al. (2023). Global water use efficiency saturation due to increased vapor pressure deficit. *Science* 381, 672–677. doi: 10.1126/science.adf5041

Liao, Z., Fei, X.-H., Zhou, B., Zhu, J., Jia, H., Chen, W., et al. (2024). Spatiotemporal variation and response of gross primary productivity to climate factors in forests in Qiannan state from 2000 to 2020. *Front. Forests Global Change* 7. doi: 10.3389/ffgc.2024.1293541

Liu, Z., Fu, Y. H., Chen, D., Crowther, T. W., Ding, R., Hao, F., et al. (2025). Increased early-season productivity drives earlier peak of vegetation photosynthesis across the Northern Hemisphere. *Commun. Earth Environ.* 6, 157. doi: 10.1038/s43247-025-02104-8

Liu, L., Gudmundsson, L., Hauser, M., Qin, D., Li, S., and Seneviratne, S. I. (2020b). Soil moisture dominates dryness stress on ecosystem production globally. *Nat. Commun.* 11, 4892. doi: 10.1038/s41467-020-18631-1

Liu, D., Lu, Q., Jiang, T., and Liu, Z. (2020a). The response characteristics of NDVI with different vegetation cover types to temperature and precipitation in China. *Ecol. Environ. Sci.* 29, 23–34. doi: 10.16258/j.cnki.1674-5906.2020.01.003

Liu, Y., Wu, C., Wang, X., Jassal, R. S., and Gonsamo, A. (2021b). Impacts of global change on peak vegetation growth and its timing in terrestrial ecosystems of the continental US. *Global Planetary Change* 207, 103657. doi: 10.1016/j.gloplacha.2021.103657

Liu, J., Zhou, T., Luo, H., Liu, X., Yu, P., Zhang, Y., et al. (2021a). Diverse roles of previous years' Water conditions in gross primary productivity in China. *Remote Sens.* 13, 58. doi: 10.3390/rs13010058

López, J., Way, D. A., and Sadok, W. (2021). Systemic effects of rising atmospheric vapor pressure deficit on plant physiology and productivity. *Global Change Biol.* 27, 1704–1720. doi: 10.1111/gcb.15548

Lu, J., and Yan, F. (2023). The divergent resistance and resilience of forest and grassland ecosystems to extreme summer drought in carbon sequestration. *Land* 12, 1672. doi: 10.3390/land12091672

Lv, Y., Li, X., and Chi, W. (2023). Maximum gross primary productivity dominates the trend in gross primary productivity in China's deciduous forest ecosystems. *Forests* 14, 1880. doi: 10.3390/f14091880

Mei, L., Bao, G., Tong, S., Yin, S., Bao, Y., Jiang, K., et al. (2021). Elevation-dependent response of spring phenology to climate and its legacy effect on vegetation growth in the mountains of northwest Mongolia. *Ecol. Indic.* 126, 107640. doi: 10.1016/j.ecolind.2021.107640

Meng, F., Liu, D., Wang, Y., Wang, S., and Wang, T. (2023a). Negative relationship between photosynthesis and late-stage canopy development and senescence over Tibetan Plateau. *Global Change Biol.* 29, 3147–3158. doi: 10.1111/gcb.16668

Meng, F., Luo, M., Wang, Y., Sa, C., Bao, S., Bao, Y., et al. (2023b). Revisiting the main driving factors influencing the dynamics of gross primary productivity in the Mongolian Plateau. *Agric. For. Meteorology* 341, 109689. doi: 10.1016/j.agrformet.2023.109689

Myneni, R. B., Keeling, C. D., Tucker, C. J., Asrar, G., and Nemani, R. R. (1997). Increased plant growth in the northern high latitudes from 1981 to 1991. *Nature* 386, 698–702. doi: 10.1038/386698a0

Niu, Z., Wang, L., Fang, L., Li, J., and Yao, R. (2020). Spatiotemporal variations in monthly relative humidity in China based on observations and CMIP5 models. *Int. J. Climatology* 40, 6382–6395. doi: 10.1002/joc.6587

Olano, J. M., Sangüesa-Barreda, G., García-López, M. A., García-Hidalgo, M., Rozas, V., García-Cervigón, A. I., et al. (2023). Water use efficiency and climate legacies dominate beech growth at its rear edge. *J. Ecol.* 111, 2160–2171. doi: 10.1111/1365-2745.14164

Peng, J., Tang, J., Xie, S., Wang, Y., Liao, J., Chen, C., et al. (2024). Evidence for the acclimation of ecosystem photosynthesis to soil moisture. *Nat. Commun.* 15, 9795. doi: 10.1038/s41467-024-54156-7

Piao, S., Wang, X., Park, T., Chen, C., Lian, X., He, Y., et al. (2020). Characteristics, drivers and feedbacks of global greening. *Nat. Rev. Earth Environ.* 1, 14–27. doi: 10.1038/s43017-019-0001-x

Rehfeldt, G. E., and Jaquish, B. C. (2010). Ecological impacts and management strategies for western larch in the face of climate-change. *Mitigation Adaptation Strategies Global Change* 15, 283–306. doi: 10.1007/s11027-010-9217-2

Richardson, A. D., Andy Black, T., Ciais, P., Delbart, N., Friedl, M. A., Gobron, N., et al. (2010). Influence of spring and autumn phenological transitions on forest ecosystem productivity. *Philos. Trans. R. Soc. B: Biol. Sci.* 365, 3227–3246. doi: 10.1098/rstb.2010.0102

Sala, O. E., Gherardi, L. A., Reichmann, L., Jobbágy, E., and Peters, D. (2012). Legacies of precipitation fluctuations on primary production: theory and data synthesis. *Philos. Trans. R. Soc. B: Biol. Sci.* 367, 3135–3144. doi: 10.1098/rstb.2011.0347

Sato, H., Kumagai, T.o., Takahashi, A., and Katul, G. G. (2015). Effects of different representations of stomatal conductance response to humidity across the African continent under warmer CO2-enriched climate conditions. *J. Geophysical Research: Biogeosciences* 120, 979–988. doi: 10.1002/2014JG002838

Sen, P. K. (1968). Estimates of the regression coefficient based on Kendall's Tau. *J. Am. Stat. Assoc.* 63, 1379–1389. doi: 10.1080/01621459.1968.10480934

Shen, X., Shen, M., Wu, C., Peñuelas, J., Ciais, P., Zhang, J., et al. (2024b). Critical role of water conditions in the responses of autumn phenology of marsh wetlands to climate change on the Tibetan Plateau. *Global Change Biol.* 30, e17097. doi: 10.1111/gcb.17097

Shen, W., Yuan, S., Jiaguo, L., Hongsheng, Z., Zhi, D., and Tang, X. (2024a). Monitoring spatio-temporal dynamics of multi-dimensional karst ecosystem quality in Southwest China by integrating multi-source data. *Int. J. Digital Earth* 17, 2356119. doi: 10.1080/17538947.2024.2356119

Shi, L., Lin, Z., Wei, X., Peng, C., Yao, Z., Han, B., et al. (2022). Precipitation increase counteracts warming effects on plant and soil C:N:P stoichiometry in an alpine meadow. *Front. Plant Sci.* 13. doi: 10.3389/fpls.2022.1044173

Sisheber, B., Marshall, M., Mengistu, D., and Nelson, A. (2022). Tracking crop phenology in a highly dynamical landscape with knowledge-based Landsat–MODIS data fusion. *Int. J. Appl. Earth Observation Geoinformation* 106, 102670. doi: 10.1016/j.jag.2021.102670

Song, L., Li, M., Xu, H., Guo, Y., Wang, Z., Li, Y., et al. (2021). Spatiotemporal variation and driving factors of vegetation net primary productivity in a typical karst area in China from 2000 to 2010. *Ecol. Indic.* 132, 108280. doi: 10.1016/j.ecolind.2021.108280

Sun, R. Y., L., Q., Niu, C. J., and Lou, A. R. (2002). *Basic Ecology* (Beijing: Higher Education Press).

Wang, Z., Cao, S., Cao, G., and Lan, Y. (2021). Effects of vegetation phenology on vegetation productivity in the Qinghai Lake Basin of the Northeastern Qinghai–Tibet Plateau. *Arabian J. Geosciences* 14, 1030. doi: 10.1007/s12517-021-07440-5

Wang, L., Li, P., Peng, Y., Ren, P., Chen, Y., Zhou, X., et al. (2025). The widely increasing sensitivity of vegetation productivity to phenology in northern middle and high latitudes. *Geophysical Res. Lett.* 52, e2024GL113892. doi: 10.1029/2024GL113892

Wang, S., Li, R., Wu, Y., and Zhao, S. (2022a). Effects of multi-temporal scale drought on vegetation dynamics in Inner Mongolia from 1982 to 2015, China. *Ecol. Indic.* 136, 108666. doi: 10.1016/j.ecolind.2022.108666

Wang, Y., Wang, Y., Tang, Y., and Zhu, X.-G. (2022b). Stomata conductance as a goalkeeper for increased photosynthetic efficiency. *Curr. Opin. Plant Biol.* 70, 102310. doi: 10.1016/j.pbi.2022.102310

Wang, X., and Wu, C. (2019). Estimating the peak of growing season (POS) of China's terrestrial ecosystems. *Agric. For. Meteorology* 278, 107639. doi: 10.1016/j.agrformet.2019.107639

Wang, S., Zhang, B., Yang, Q., Chen, G., Yang, B., Lu, L., et al. (2017). Responses of net primary productivity to phenological dynamics in the Tibetan Plateau, China. *Agric. For. Meteorology* 232, 235–246. doi: 10.1016/j.agrformet.2016.08.020

White, M.a., De Beurs, K.m., Didan, K., Inouye, D.w., Richardson, A.d., Jensen, O.p., et al. (2009). Intercomparison, interpretation, and assessment of spring phenology in North America estimated from remote sensing for 1982–2006. *Global Change Biol.* 15, 2335–2359. doi: 10.1111/j.1365-2486.2009.01910.x

Wu, G.-L., Cheng, Z., Alatalo, J. M., Zhao, J., and Liu, Y. (2021). Climate warming consistently reduces grassland ecosystem productivity. *Earth's Future* 9, e2020EF001837. doi: 10.1029/2020EF001837

Wu, L., Zhang, Y., Luo, G., Chen, D., Yang, D., Yang, Y., et al. (2023). Characteristics of vegetation carbon sink carrying capacity and restoration potential of China in recent 40 years. *Front. Forests Global Change Volume* 6. doi: 10.3389/ffgc.2023.1266688

Wu, D., Zhao, X., Liang, S., Zhou, T., Huang, K., Tang, B., et al. (2015). Time-lag effects of global vegetation responses to climate change. *Global Change Biol.* 21, 3520–3531. doi: 10.1111/gcb.12945

Xia, J., Niu, S., Ciais, P., Janssens, I. A., Chen, J., Ammann, C., et al. (2015). Joint control of terrestrial gross primary productivity by plant phenology and physiology. *Proc. Natl. Acad. Sci.* 112, 2788–2793. doi: 10.1073/pnas.1413090112

Xiao, J., Wang, Z., Sun, W., Li, S., Han, F., Huang, S., et al. (2023). The relative effects of climate change and phenological change on net primary productivity vary with grassland types on the Tibetan Plateau. *Remote Sens.* 15, 3733. doi: 10.3390/rs15153733

Xie, Z., Zhu, W., Qiao, K., Li, P., and Liu, H. (2021). Joint influence mechanism of phenology and climate on the dynamics of gross primary productivity: insights from temperate deciduous broadleaf forests in North America. *J. Geophysical Research: Biogeosciences* 126, e2020JG006049. doi: 10.1029/2020JG006049

Xu, Y., Xuejian, L., Huaqiong, D., Fangjie, M., Guomo, Z., Zihao, H., et al. (2023). Spatiotemporal variation in bamboo Solar-induced chlorophyll fluorescence (SIF) in China based on the global Orbiting Carbon Observatory-2 (OCO-2) carbon satellite and study on the response to climate and terrain. *GIScience Remote Sens.* 60, 2253952. doi: 10.1080/15481603.2023.2253952

Xu, Y., Z., z.-W., Meng, Y.-C., Pan, Y.-C., Guo, Z.-D., and Zhang, Y. (2024). Spatio-temporal variation in net primary productivity of different vegetation types and its influencing factors exploration in southwest China. *Environ. Sci.* 45, 262–274. doi: 10.13227/j.hjkx.202207068

Xu, R., Zhang, J., Chen, F., Yu, B., Ali, S., Ullah, H., et al. (2024). Quantitative assessment of spatiotemporal variations and drivers of gross primary productivity in tropical ecosystems at higher resolution. *Int. J. Appl. Earth Observation Geoinformation* 135, 104248. doi: 10.1016/j.jag.2024.104248

Xu, L., Zhang, X., Wang, Y., Fu, Y., Yan, H., Qian, S., et al. (2021). Drivers of phenology shifts and their effect on productivity in northern grassland of China during 1984–2017—evidence from long-term observational data. *Int. J. Biometeorology* 65, 527–539. doi: 10.1007/s00484-020-02046-0

Yan, P., He, N., Fernández-Martínez, M., Yang, X., Zuo, Y., Zhang, H., et al. (2025). Plant acquisitive strategies promote resistance and temporal stability of semiarid grasslands. *Ecol. Lett.* 28, e70110. doi: 10.1111/ele.70110

Yang, F., Liu, C., Chen, Q., Lai, J., and Liu, T. (2024). Earlier spring-summer phenology and higher photosynthetic peak altered the seasonal patterns of vegetation productivity in alpine ecosystems. *Remote Sens.* 16, 1580. doi: 10.3390/rs16091580

Yang, J., Zhang, X. C., Luo, Z. H., and Yu, X. J. (2017). Nonlinear variations of net primary productivity and its relationship with climate and vegetation phenology, China. *Forests* 8, 361. doi: 10.3390/f8100361

Yao, Y., Wang, X., Li, Y., Wang, T., Shen, M., Du, M., et al. (2018). Spatiotemporal pattern of gross primary productivity and its covariation with climate in China over the last thirty years. *Global Change Biol.* 24, 184–196. doi: 10.1111/gcb.13830

Ye, L., Cheng, L., Liu, P., Liu, D., Zhang, L., Qin, S., et al. (2021). Management of vegetative land for more water yield under future climate conditions in the over-utilized water resources regions: A case study in the Xiong'an New area. *J. Hydrology* 600, 126563. doi: 10.1016/j.jhydrol.2021.126563

Yuan, W., Zheng, Y., Piao, S., Ciais, P., Lombardozzi, D., Wang, Y., et al. (2019). Increased atmospheric vapor pressure deficit reduces global vegetation growth. *Sci. Adv.* 5, eaax1396. doi: 10.1126/sciadv.aax1396

Zhang, Y., Fang, L., and Jing, P. (2020). Analysis of broad leaved forest carbon sinks changes and forest economics and management in China. *Environ. Sci. pollut. Res.* 27, 12922–12931. doi: 10.1007/s11356-019-05772-0

Zhang, J., Gonsamo, A., Tong, X., Xiao, J., Rogers, C. A., Qin, S., et al. (2023). Solar-induced chlorophyll fluorescence captures photosynthetic phenology better than traditional vegetation indices. *ISPRS J. Photogrammetry Remote Sens.* 203, 183–198. doi: 10.1016/j.isprsjprs.2023.07.021

Zhang, P., Yang, X., Chen, Y., Wei, Z., and Liu, F. (2021). Dissecting the combined effects of air temperature and relative humidity on water-use efficiency of barley under drought stress. *J. Agron. Crop Sci.* 207, 606–617. doi: 10.1111/jac.12475

Zhao, M., Heinsch, F. A., Nemani, R. R., and Running, S. W. (2005). Improvements of the MODIS terrestrial gross and net primary production global data set. *Remote Sens. Environ.* 95, 164–176. doi: 10.1016/j.rse.2004.12.011

Zhao, W., Hu, Z., Guo, Q., Wu, G., Chen, R., and Li, S. (2019). Contributions of climatic factors to inter-annual variability of vegetation index in northern China grasslands. *J. Climate* 33, 175–183. doi: 10.1175/JCLI-D-18-0587.1

Zhou, Y. (2020). Relative contribution of growing season length and amplitude to long-term trend and interannual variability of vegetation productivity over northeast China. *Forests* 11, 112. doi: 10.3390/f11010112

Zu, J., Zhang, Y., Huang, K., Liu, Y., Chen, N., and Cong, N. (2018). Biological and climate factors co-regulated spatial-temporal dynamics of vegetation autumn phenology on the Tibetan Plateau. *Int. J. Appl. Earth Observation Geoinformation* 69, 198–205. doi: 10.1016/j.jag.2018.03.006